Chapter 35

TMV-Based Adapter Templates for Enhanced Enzyme Loading in Biosensor Applications

Claudia Koch, Arshak Poghossian, Christina Wege, and Michael J. Schöning

Abstract

Nanotubular tobacco mosaic virus (TMV) particles and RNA-free lower-order coat protein (CP) aggregates have been employed as enzyme carriers in different diagnostic layouts and compared for their influence on biosensor performance. In the following, we describe a label-free electrochemical biosensor for improved glucose detection by use of TMV adapters and the enzyme glucose oxidase (GOD). A specific and efficient immobilization of streptavidin-conjugated GOD ([SA]-GOD) complexes on biotinylated TMV nanotubes or CP aggregates was achieved via bioaffinity binding. Glucose sensors with adsorptively immobilized [SA]-GOD, and with [SA]-GOD cross-linked with glutardialdehyde, respectively, were tested in parallel on the same sensor chip. Comparison of these sensors revealed that TMV adapters enhanced the amperometric glucose detection remarkably, conveying highest sensitivity, an extended linear detection range and fastest response times. These results underline a great potential of an integration of virus/biomolecule hybrids with electronic transducers for applications in biosensorics and biochips. Here, we describe the fabrication and use of amperometric sensor chips combining an array of circular Pt electrodes, their loading with GOD-modified TMV nanotubes (and other GOD immobilization methods), and the subsequent investigations of the sensor performance.

Key words Tobacco mosaic virus (TMV), Coat protein, Enzyme nanocarrier, Glucose biosensor, Glucose oxidase, Amperometric sensor, Pt electrode array, Streptavidin–biotin

1 Introduction

Enzyme activity may be affected to a critical extent upon immobilization on solid supports, which is, however, advantageous or necessary for numerous applications, including many biosensor layouts. The choice of the right immobilization strategy is therefore essential for the generation of biosensors with good and reliable performance, storage stability, and reusability. The efficiency of enzyme immobilization is of equal importance, since a high level of immobilization results in a good cost–benefit ratio. The immobilization method of choice should further allow strong attach-

Christina Wege and George P. Lomonossoff (eds.), *Virus-Derived Nanoparticles for Advanced Technologies: Methods and Protocols*, Methods in Molecular Biology, vol. 1776, https://doi.org/10.1007/978-1-4939-7808-3_35,

ment to the detector surfaces, to avoid unwanted detachment during measurements. Concomitantly, however, the surface-coupled enzymes need to maintain their structure and thus catalytic activity, which must not be hindered by the coupling process. To reach these goals, a broad spectrum of different immobilization techniques has been reported in the literature, including cross-linking, covalent or affinity binding, physical adsorption, entrapment, and various linker-based strategies (refer to reviews such as [1–5] for further details).

Recently, the coupling of (bio)chemical recognition elements with multivalent nanoscale biological building blocks, such as virus particles, has been found to be a very promising strategy for the creation of biohybrids; these open up novel opportunities for the high-density presentation of enzymes [6–12]. One of the most promising viral backbones is the plant virus tobacco mosaic virus (TMV) [13–15]. TMV is a rigid nanotube with a length of 300 nm and an outer diameter of 18 nm. Native TMV consists of 2130 identical coat protein (CP) subunits which self-assemble into a helical structure embedding a single-stranded RNA genome [16, 17]. Numerous studies have demonstrated the huge potential of the robust TMV particles as versatile building blocks for functional materials and as high-yield nanotemplates, allowing the presentation of active molecules or synthetic compounds (*see* Fig. 1) [18].

Recently, TMV has successfully been introduced as enzyme carrier scaffold in a new approach for the improvement of label-free glucose biosensors [6]. In this study, enzyme coupling to the TMV capsid was achieved by a cysteine-modified TMV CP variant (TMV_{Cys}) [19], yielding versatile carrier rods with more than 2000 selectively addressable thiols (also described in Chapter 27). The thiol group of a cysteine exposed on the surface of every CP subunit allowed the coupling of bifunctional maleimide-PEG-biotin linkers, resulting in biotinylated TMV-based nanoparticles (TMV_{Cys}/Bio). Streptavidin-conjugated glucose oxidase ([SA]-GOD) was immobilized via biotin–streptavidin affinity interaction on the surface of the TMV_{Cys}/Bio rods, or of RNA-free CP_{Cys}/Bio aggregates (ring-shaped "disks" and lower order oligomers) produced from the biotinylated rods, respectively (*see* also [7]). The affinity binding method allowed control over the bioactive molecules' orientation, in order to avoid enzyme deactivation and/or blocking of their active sites [20]. The TMV-based adapter templates were then adsorbed on sensor surfaces, thereby allowing the immobilization of enzymes at high surface densities in the detector devices. For comparison, glucose sensors with adsorptively immobilized [SA]-GOD, as well as [SA]-GOD cross-linked with glutardialdehyde (techniques often used for enzyme immobilization on sensors) were tested in parallel. Physical adsorption is a simple way to immobilize enzymes without substantial loss of their activity. However, a weak bond between the sensor surface and the enzyme

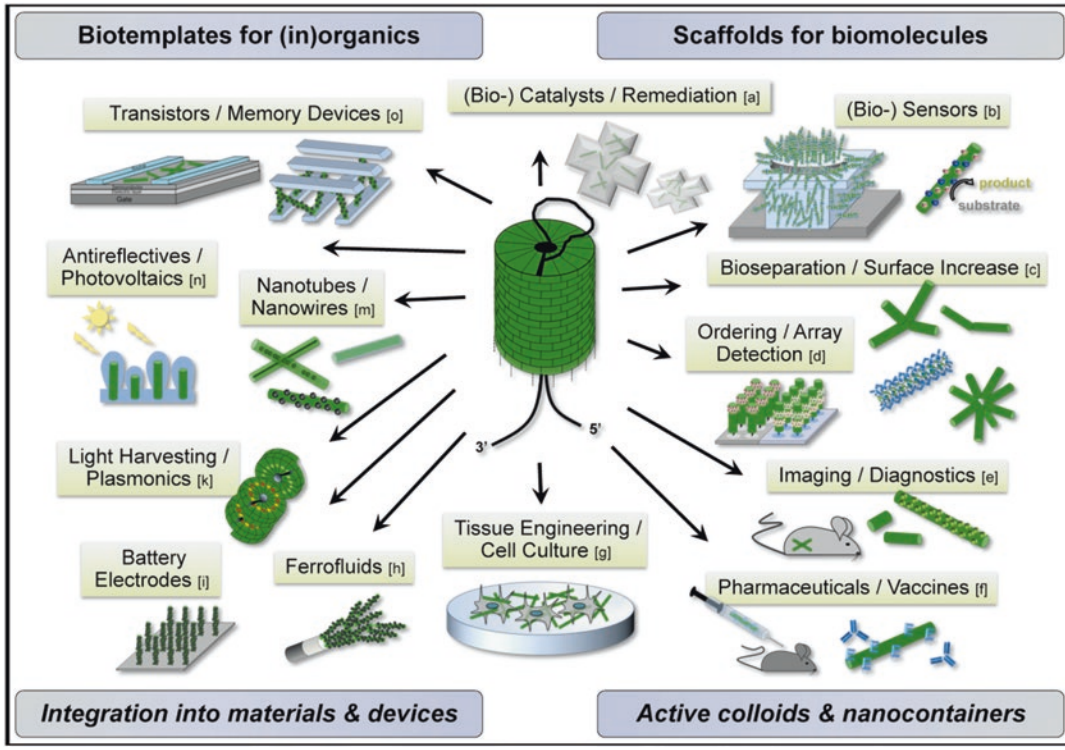

Fig. 1 TMV as a versatile multivalent soft-matter template: TMV and related tobamoviruses are used as templates for the construction of various biohybrid nanoobjects and nanostructured materials. For references (**a**–**o**) ***see*** original work [18]. Reproduced according to the Creative Commons Attribution 2.0 International Public License from [18]

can lead to a fast leakage of the enzymes. An immobilization by cross-linking with glutardialdehyde or other bifunctional agents is attractive due to its simplicity and the strong chemical binding between biomolecules. The main drawback is the possible loss of enzyme activity due to distortion of the enzyme conformation and chemical alteration of the active sites during cross-linking [1]. Each of these immobilization strategies was used to immobilize [SA]-GOD conjugates on one out of four single Pt electrodes on the same sensor chip, followed by amperometric detection of varying glucose concentrations. An exemplary distribution of electrodes (glucose sensors) on the chip with the differently immobilized [SA]-GOD conjugates is summarized in Fig. 2.

Comparable studies in ELISA-plate wells showed that by using these viral adapters, considerably higher amounts of enzymes could be installed from commercial [SA]-GOD preparations than through direct or biotin linker-mediated coupling. This resulted in up to 45 times higher turnover rates, increased reusability ($t_{50\%}$ = 13 days instead of 4–6 days) as well as enhanced stability ($t_{50\%}$ = 3 weeks instead of 1 week) compared to conventionally

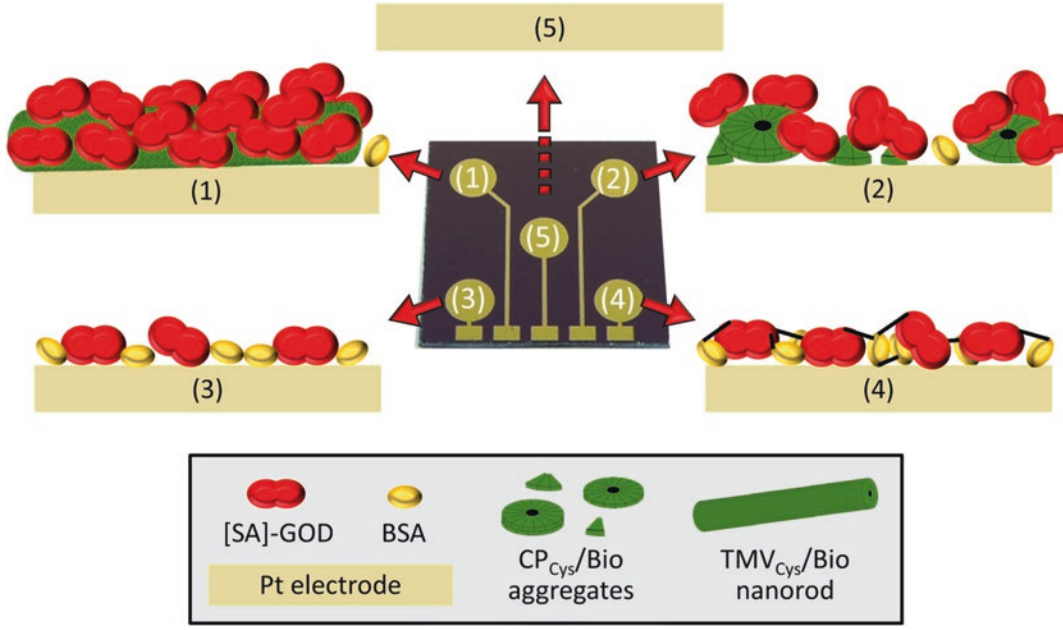

Fig. 2 Example of electrode loading with [SA]-GOD from a BSA-containing stock solution in different layouts. Shown is an array of Pt electrodes loaded with [SA]-GOD-modified TMV nanotubes (1) or CP aggregates (2), adsorptively immobilized [SA]-GOD (3) as well as [SA]-GOD cross-linked with glutardialdehyde (4), all subjected to enzyme loading in the presence of BSA. A bare electrode (5) serves for electrochemical functionality testing of the as-produced electrodes

bound enzymes, indicating a stabilizing effect of the TMV environment over weeks [7]. In the amperometric detection setup, Pt electrodes of electrochemical sensor chips loaded with [SA]-GOD-modified TMV sticks exhibited faster response times ($t_{90\%}$ = 5 s), higher glucose sensitivities (4.9 nA/mM mm^2), an extended nearly linear detection range (0.1–7.4 mM glucose concentration), and less noise signal compared to sensors using other immobilization methods (for typical response curves *see* Fig. 3) [6] (*see* **Note 1**).

Taken together, these results underline a great potential for the integration of TMV as enzyme carrier in sensing devices. Despite the observed benefits (higher enzyme loading, better sensor stability and faster response times), there are up to now only few reports on using TMV particles as scaffolds in sensing applications (*see* e.g. [15, 21] and references therein). In combination with inorganic materials, TMV nanoparticles coated with palladium as a sensing material have promoted the development of a surface acoustic wave (SAW) hydrogen sensor [22]. Using organically modified TMV nanorods, it was possible to create a thin film sensor for the detection of volatile organic compounds (VOC) such as ethanol and methanol, after deposition of oligo-aniline-grafted TMV particles onto a glass substrate [23]. Another biosensor approach is based on TMV-like particles modified with 2,4,6-trinitrotoluene-

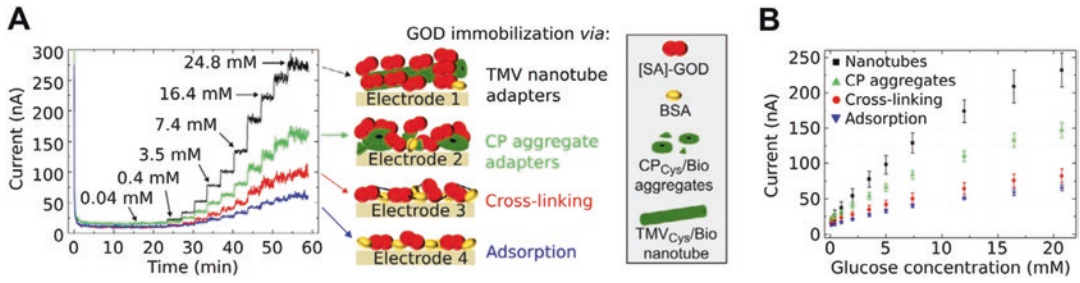

Fig. 3 Dynamic responses (**a**) and mean calibration curves (**b**) of four glucose sensors with variously immobilized [SA]-GOD conjugates on the same chip, recorded in solutions with different glucose concentrations. Reproduced according to the Creative Commons Attribution 2.0 International Public License from [6]

(TNT)-binding peptides for sensing in solution [24]. Recently, it was shown that the combination of a novel TMV-VLP receptor layer for antibody binding with an optical microdisk resonator can be used as transducer for biosensing applications [25].

The following protocol will focus on a recently established label-free biosensor layout profiting from biotinylated TMV-based adapter templates for the efficient and durable installation of the glucose sensor enzyme GOD on the surface of sensor electrodes for amperometric readout [6]. It describes the preparation of biotin-fashioned TMV-based adapters (both nanosticks and CP aggregates) and the fabrication of appropriate sensor electrodes, TMV adapter immobilization on their surfaces, their equipment with [SA]-GOD via bioaffinity coupling and, finally, proof-of-concept measurements demonstrating the glucose detection capabilities of the system in comparison to control layouts.

2 Materials

Prepare all buffers and solutions with deionized water (ddH_2O, 18.3 MΩ cm; e.g., purified by a membraPure system (Aquintus) or other comparable water quality) if not stated otherwise. Prepare all virus dilutions in 10 mM sodium potassium phosphate (SPP) pH 7.0, if not otherwise recommended. Dissolve all virus-containing pellets in 10 mM SPP pH 7.0.

2.1 Biotin Linker Coupling to TMV_{Cys} Nanosticks [7]

1. 10 mM sodium potassium phosphate (SPP) buffer pH 7.0: Mix 10 mM NaH_2PO_4 and 10 mM K_2HPO_4 until a pH of 7.0 is obtained.
2. 15 mg TMV_{Cys} [19] in SPP: Use a virus particle preparation of typically 5 mg/ml isolated from about 20 g leaves of systemically infected *Nicotiana tabacum* 'Samsun' nn plants (*see* for example Subheading 2.3 in Chapter 27).

3. Maleimide-activated biotin linker to enable high-affinity binding of [SA]-GOD conjugates (maleimide-PEG_{11}-biotin EZ-Link®, Thermo Scientific) (*see* **Note 2**).
4. Dimethyl sulfoxide (DMSO), anhydrous, >99.9%.
5. Highly accurate balance.
6. Ultracentrifuge with fixed-angle rotor holding small tubes (up to 1.5 ml) and capable of running at 120,000 × *g* [e.g., Optima L-80 XP Ultracentrifuge (Beckmann Coulter) and rotor 45 Ti (Beckmann Coulter)].
7. 1.5 ml tubes suitable for ultracentrifugation (UC).
8. UV–Vis spectrophotometer [e.g., NanoDrop ND-1000 spectrophotometer (Thermo Scientific)] or equivalent instrument capable of measuring the UV absorption of small volumes (e.g., 1–2 µl).
9. SDS–polyacrylamide electrophoresis (SDS-PAGE) equipment and solutions for discontinuous Laemmli gels with a 4% stacking gel and 15% separation gel, as for example listed in Subheading 2.5 of Chapter 23.
10. Coomassie Brilliant Blue R-250 and destaining solution or similar standard staining solution for SDS-PAGE.
11. ImageJ by Rasband, W.S., US National Institutes of Health, Bethesda, Maryland, USA; software can be downloaded from https://imagej.nih.gov/ij/download.html.
12. Standard molecular biology instrumentation and consumables such as microliter pipettes and microcentrifuge tubes.

2.2 CP_{Cys}/Bio Preparation

1. 1 ml of a 5 mg/ml TMV_{Cys}/Bio solution (produced in Subheading 3.1).
2. Ice-cold glacial acetic acid.
3. Centrifuge with fixed angle rotor holding small tubes (up 2 ml) and capable of running at 20,000 × *g* and 4 °C.
4. Dialysis tubing: 8 kDa molecular weight cutoff (MWCO) (e.g., Spectra/Por® 7 Dialysis Membrane Pretreated RC Tubing, Spectrum Laboratories, Inc., Rancho Dominguez, CA, USA).
5. Two clips, suitable to block the tubing.
6. 3 × 5 l ddH_2O at 4 °C.
7. 10 mM SPP, pH 7.0.
8. UV–Vis spectrophotometer [e.g., NanoDrop ND-1000 spectrophotometer (Thermo Scientific)] or equivalent instrument capable of measuring the UV absorption of small volumes (e.g., 1–2 µl).

2.3 Sensor Chip Fabrication [26]

1. UNIVEX 350 Evaporator System (Leybold/Oerlikon) for electron-beam evaporation.
2. Photoresist (AZ 5214, MicroChemicals GmbH); a light-sensitive material used in photolithography to form a patterned coating on a surface.
3. Ultrasonic wedge bonder (Kulicke & Soffa Pte Ltd).
4. Silicone rubber (Momentive Performance Materials GmbH, Germany) for encapsulation of bond pads and bond wires.
5. Printed circuit boards: homemade (FH Aachen, Germany).
6. Oxidation furnace (Tempress, Netherlands) for thermal oxidation of Si wafer.
7. p-type Si wafer (Topsil GlobalWafers, thickness: 356–406 μm; specific resistivity: ~1000 Ω cm; polished).
8. Photomask for opening windows for deposition of metal layers.
9. Mask Aligner for lithography (MJB3, Suss Microtec, Germany); UV-radiation: 10 mW/cm^2, λ = 365 nm.
10. Titanium (Umicore, granules).
11. Platinum (Umicore, granules).
12. Acetone (Technic France).
13. Liquid glue to connect chip and board.

2.4 Sensor Chip Loading with Viral Adapters and Immobilization of [SA]-GOD

1. 10 mM SPP, pH 7.0.
2. 0.33 μg/μl TMV_{Cys}/Bio and 0.33 μg/μl CP_{Cys}/Bio in 10 mM SPP pH 7.0: dilute prepared TMV_{Cys}/Bio (Subheading 3.1) and CP_{Cys}/Bio solutions (Subheading 3.2) in 10 mM SPP pH 7.0.
3. Humid chamber to avoid evaporation of protein solutions.
4. Streptavidin-conjugated glucose oxidase ([SA]-GOD; 1 μg/μl in storage buffer (0.1 M K-phosphate buffer pH 6.0, supplemented with 10 μg/μl BSA (bovine serum albumin) and 1200 ppm 5-nitro-5-bromo-1,3-dioxane)) with 1–2 [SA] partners per GOD (provided by the supplier SDT, Baesweiler, Germany).
5. 2% (w/v) glutardialdehyde [diluted from 25% (w/v) glutardialdehyde solution in water (Merck)].

2.5 Electrochemical Characterization of Sensor Electrodes

1. 250 mM glucose (glucose stock solution).
2. Measuring vessel with holder able to bear two sensor chips boards in parallel.
3. 10 mM SPP, pH 7.0.

4. Potentiostat (PalmSens, Palm Instruments BV) equipped with an eight-channel multiplexer (CH8, Palm Instruments BV) to switch between the individual channels.
5. Liquid-junction Ag/AgCl reference electrode (3 M KCl, Metrohm).
6. Pt counter electrode with a surface area of approximately 1 cm.
7. Dark Faraday cage of approximately 60 × 40 × 30 cm: home-made (FH Aachen, Germany).
8. Software: PSTrace (PalmSens, PalmSens BV).

3 Methods

Carry out all processes and preparation steps at room temperature (RT), unless otherwise specified.

3.1 TMV_{Cys} Isolation and Biotin Linker Coupling

1. Dilute a stock solution of TMV_{Cys} particles from infected *N. tabacum* leaves (isolated according to Gooding and Herbert [27] as described in detail in Chapter 23 or 27) to yield a total of 3 ml TMV_{Cys} of 5 mg/ml in 10 mM SPP buffer pH 7.0 (*see* **Note 3**).
2. Divide the maleimide-PEG_{11}-biotin linker in small packages of around 5 mg each and freshly dissolve one dose prior to the experiment in DMSO (f.c. 250 nmol/µl). Store the dissolved linker solution at 4 °C.
3. Mix 10 mg TMV_{Cys} (i.e., 2 ml of **step 1**) with 12 µmol (i.e., 5 µl stock solution) linker and incubate under gentle agitation at RT for 16 h (*see* **Note 4**).
4. Split the TMV_{Cys} and linker containing solution in equal parts and transfer them into tubes suitable for ultracentrifugation (UC).
5. Remove unbound maleimide-biotin linker molecules by UC (120,000 × *g*, 4 °C, 2 h): collect the supernatants with nonreacted linkers by use of a pipette and discard them. Resuspend UC pellets containing the linker-fashioned virus particles (TMV_{Cys}/Bio) in the initial amount of the TMV solution (here: 1 ml for each tube) in 10 mM SPP (pH 7.0) and combine both portions.
6. Determine the TMV concentration using a spectrophotometer and the extinction coefficient for TMV at 260 nm (ε_{260} = 3 ml/(mg•cm) [28]) (*see* **Note 5**).
7. Analyze the samples on a discontinuous Laemmli SDS-PA gel according to standard methods [29]. Prepare a 15% separation gel with a 4% stacking gel. Mix 1.5 µg of the TMV_{Cys}/Bio sample with SDS-gel loading buffer freshly supplemented with

reducing agent (dithiothreitol, β-mercaptoethanol or similar) to obtain a final volume of 10 µl. Heat for 5 min at 95 °C, load samples and a protein molecular weight marker into the slots and perform the electrophoresis. After disassembly of the SDS-PAGE setup, fix and stain the gel with Coomassie Blue R250 or a similar colloidal dye according to standard methods (for details on SDS-PAGE, you may also refer for example to Chapter 23, Subheading 3.3.1). After destaining of the gel background and the appearance of clear bands, document the image and use ImageJ (or a different suitable image analysis software) to assess the percentage of TMV CPs carrying a linker molecule (*see* Fig. 4 and **Note 6**).

3.2 CP_{Cys}/Bio Preparation from TMV_{Cys}/Bio Particles

1. Mix 1 Vol. TMV_{Cys}/Bio suspension (from Subheading 3.1, **step 6**; typically 600 µl) with 2× Vol. ice-cold glacial acetic acid [30]. Incubate for 20 min on ice. To separate RNA and CPs, centrifuge at 20,000 × *g* at 4 °C for 20 min. Collect the supernatant containing the CPs.
2. Incubate a ~10 cm long piece of dialysis tubing (8 kDa MWCO) for 2 min in ultrapure water. Block one end of the tubing with a clip. Transfer the supernatant into the dialysis tubing and block the second end with a clip.
3. Dialyze against ultrapure water (~ 5 l ddH_2O) for 24–48 h at 4 °C until the tubing content seems cloudy or turbid. Change water every few hours.

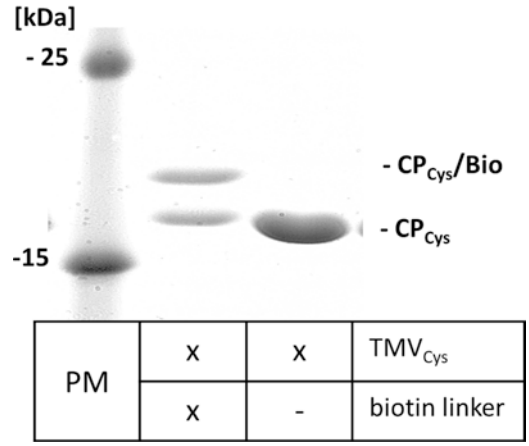

Fig. 4 Biotinylation of TMV_{Cys} behind Cyscoupling of maleimide-PEG_{11}-biotin (biotin linker) to the thiol groups of TMV_{Cys} (CP_{Cys}) results in a shift of the CP signal (CP_{Cys}/Bio). Samples were analyzed using a 15% SDS-PA gel. CPs were stained with Coomassie Brilliant Blue R250. Image evaluation using ImageJ revealed a coupling efficiency of approximately 50%

4. Transfer content into a 15 ml tube and subsequently divide the solution into 1.5 ml microcentrifuge tubes and centrifuge at 20,000 × *g* at 4 °C for 20 min.
5. Discard the supernatant and dissolve the CP_{Cys}/Bio-containing pellet in 10 mM SPP, pH 7.0 [total volume of all pellets: ½ Vol. of the initial TMV solution (here: 300 µl)]. Combine the resuspended pellets. Store at RT (or at 4 °C for prolonged storage).
6. Determine the approximate protein concentration of the CP_{Cys}/Bio solution using a spectrophotometer and the extinction coefficient for TMV CPs at 280 nm (ε_{280} = 1.3 ml/(mg•cm) [28]) (*see* **Note 7**).

3.3 Amperometric Sensor Chips Fabrication

The used chips consist of a p-Si-SiO_2-Ti-Pt layer structure. The process steps of sensor chip fabrication are described in detail in [26] and are shown in Fig. 5. Briefly:

1. Grow 500 nm SiO_2 by thermal wet oxidation on a p-Si wafer at 1100 °C for 45 min.
2. For structuring the electrode distribution on the sensor surface, use spin-coating of photoresist at 4000 min^{-1} onto the Si wafer (*see* **Note 8**).

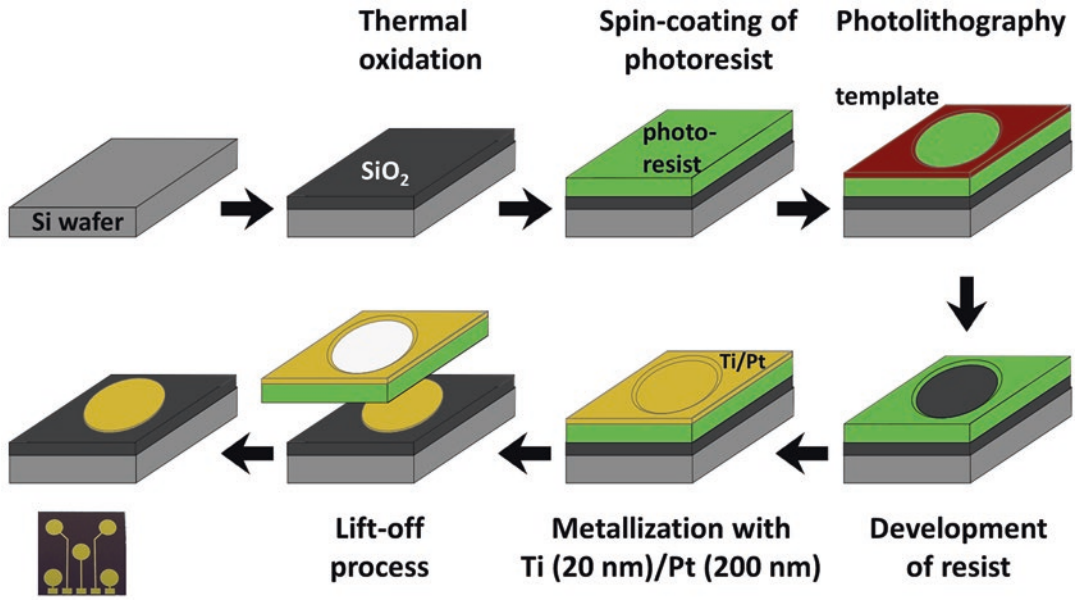

Fig. 5 Flowchart showing the fabrication steps of an amperometric sensor chip; thermal wet oxidation for insulation → deposition of photoresist layer and patterning through template (photomask) → development of resist by UV → deposition of electrode material → lift-off process of photoresist and metal layers

3. Use a template (photomask) to obtain a desired pattern on the photoresist: expose sensor with photomask to UV radiation (t = 5 s, I = 10 mW/cm^2, λ = 365 nm).
4. Deposit 20 nm titanium by electron-beam evaporation as adhesion layer on top of the SiO_2.
5. Deposit a 200 nm layer of Pt as electrode material.
6. Use acetone as solvent in the lift-off process (*see* **Note 9**).
7. Separate the processed wafer into chips of 10 mm × 10 mm. After cleaning, glue the sensor chips onto printed circuit boards.
8. Use an ultrasonic wedge bonder to provide electrical connection between sensor chip electrodes and the printed circuit boards.
9. Use silicone rubber to encapsulate the bond pads and bond wires (*see* **Note 10**).

A schematic layer structure (a), layout of Pt electrodes on a chip (b) and a photograph of a bonded and encapsulated sensor chip on a printed circuit board (c) are depicted in Fig. 6. Every chip comprises five circular working electrodes, each having a diameter of 2 mm (an area of 3.14 mm^2) and a distance to the next Pt electrode of ~2 mm to avoid cross-talk.

3.4 Sensor Chip Loading with Viral Adapters and Immobilization of [SA]-GOD

Recently published data revealed that 1 µg TMV_{Cys}/Bio sticks are sufficient to saturate an area of 2 mm diameter on the Pt surface of the electrodes [6]. To investigate the influence of the viral adapters on the biosensor performance, glucose sensors with adsorptively immobilized [SA]-GOD as well as [SA]-GOD cross-linked on the electrodes with glutardialdehyde can be tested in parallel, which enables comparative studies. An example for the possible distribution of differently immobilized [SA]-GOD conjugates is shown in Fig. 2. Since the commercial [SA]-GOD preparation contains 10 µg/µl BSA, the BSA molecules can adsorb nonspecifically and will reside in areas not exposing biotin linkers (where high-affinity binding of [SA]-GOD will replace BSA). BSA is thus also available

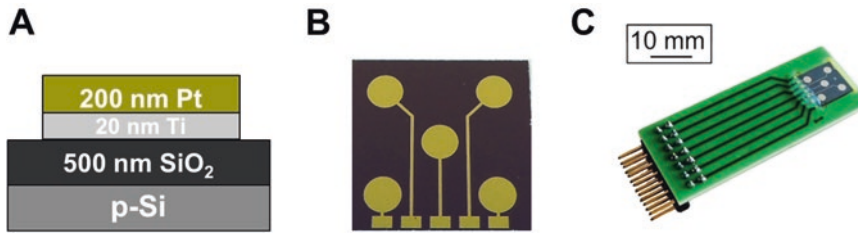

Fig. 6 Schematic layer structure (**a**), layout of Pt electrodes on a chip (**b**) and photograph of a bonded and encapsulated sensor chip on a printed circuit board (**c**)

as bridging molecule upon glutardialdehyde-mediated cross-linking.

1. Prepare for electrode (1) of the sensor chip 3 µl of TMV_{Cys}/Bio, and for electrode (2) 3 µl CP_{Cys}/Bio in 10 mM SPP buffer, respectively, with a concentration of 0.33 µg/µl each.
2. Incubate the 3 µl of TMV_{Cys}/Bio on electrode (1) and the 3 µl of CP_{Cys}/Bio on electrode (2) of one and the same sensor chip at RT for 1 h in a humid chamber (*see* **Note 11**).
3. Rinse the sensor chip thoroughly by repeated dipping in deionized (DI) water to remove nonadsorbed virus particles.
4. Mix 9 µl of [SA]-GOD solution with 6 µl 10 mM SPP buffer. Apply 5 µl of this mixture onto electrode (1) (functionalized with TMV_{Cys}/Bio), 5 µl on electrode (2) (functionalized with CP_{Cys}/Bio), and 5 µl on the so far unmodified electrode (3), respectively. Equip electrode (4) with [SA]-GOD undergoing cross-linking with both [SA]-GOD molecules and BSA by glutardialdehyde during the immobilization. To this end, mix 3 µl of [SA]-GOD solution with 2 µl cross-linker (2% glutardialdehyde; total volume 5 µl) (*see* **Note 12**). Incubate the enzyme solution on each electrode surface overnight at 4 °C in a humid chamber to allow specific bioaffinity binding of streptavidin and biotin. (The bare electrode (5) serves for electrochemical functionality testing of the as-produced electrodes.)
5. Rinse the sensor chip thoroughly by repeated dipping in deionized (DI) water to remove nonattached [SA]-GOD conjugates, BSA and unstably adsorbed virus particles or CP aggregates serving as adapter templates.

3.5 Electrochemical Characterization of Sensor Electrodes

Integrate the sensor chip loaded with variously immobilized [SA]-GOD conjugates (*see* Subheading 3.4) into the measurement setup (*see* Fig. 7).

1. Fill the measuring vessel with 10 mM SPP pH 7.0, add a magnetic stir bar and install holder on a magnetic stirrer.
2. Set the sensor chip into the holder so that the electrodes are immersed within the 10 mM SPP pH 7.0 buffer and connect the chip with the potentiostat (*see* **Note 13**).
3. Install the conventional liquid-junction Ag/AgCl reference electrode and the Pt counter electrode.
4. Apply a constant potential of +0.6 V vs. Ag/AgCl to the working electrodes (1) to (4).
5. Measure the background current of each sensor electrode in the absence of glucose for 10 min.
6. Add glucose from a 250 mM glucose stock solution to the buffer to reach a glucose concentration of 2 µM. Use the magnetic

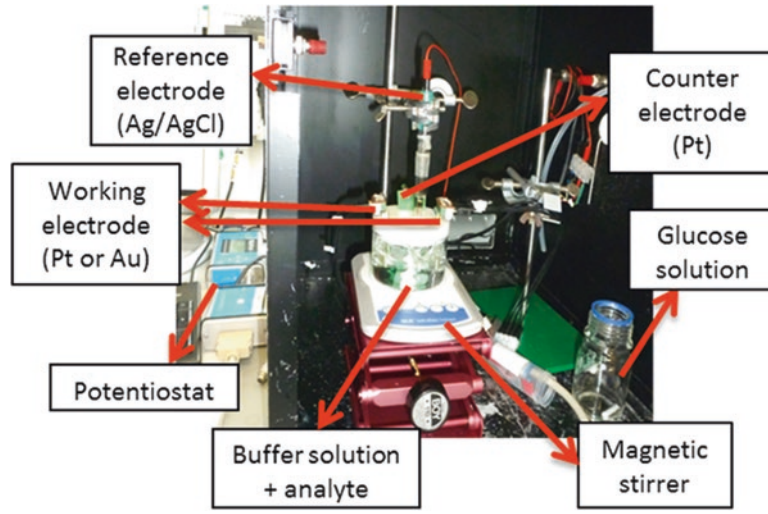

Fig. 7 Experimental setting for electrochemical characterization of amperometric glucose biosensors

stirrer to obtain a homogeneous mixture of the glucose solution.

7. Record the sensor performance of the working electrodes for 3–4 min.
8. Increase the glucose concentration in the measuring vessel sequentially by addition of more glucose from the stock solution in appropriate steps up to 25 mM glucose to the constantly stirred buffer solution. Measure the electrodes' performance after each step for 3–4 min, as described before.

As described in more detail recently [6], the presence of TMV-based adapter templates is expected to improve the performance of the respective sensor electrodes substantially, with the beneficial effects of nanostick templates surpassing those of plain CP coatings. Typical sensor response curves and the corresponding currents are shown in Fig. 3.

4 Notes

1. Explanation of some essential terms: reusability = the ability of a sensor to maintain its performance characteristics over a certain period of time; the reproducibility of output readings is determined at constant conditions; $t_{50\%}$ = the time point at which the sensor's initial performance is decreased to 50% of the original values (under constant conditions); response time = the time period during which the sensor signal reaches a specified percentage (e.g., 90%) of its final value in response to a stepwise change of the analyte concentration; sensitiv-

ity = the ratio of change in the sensor output signal to the change in the analyte concentration ≈ slope of calibration curve; nearly linear concentration range = best fit between the calibration curve and a specified straight line.

2. It is expected that these long bifunctional linkers with a total length of 6 nm provide all degrees of freedom required for a dense immobilization of enzymes on the adapters, resulting in full coverage of the TMV carrier sticks [7].
3. Store all TMV-containing solutions at 4 °C in 10 mM SPP buffer pH 7.0.
4. 10 mg TMV_{Cys} with 12 μmol linker corresponds to a 22-fold molar excess of maleimide-PEG_{11}-biotin linkers (in relation to the 2130 attachment sites on every TMV_{Cys} particle). This is sufficient to obtain TMV-based nanoscaffolds with 50–90% of the CP_{Cys} attachment sites biotinylated (in dependence on linker reactivity and coupling conditions), allowing for efficient and simple high-affinity binding of [SA]-GOD conjugates.
5. In principle, TMV particle concentration can be calculated from spectrophotometric absorption values using the Lambert-Beer-Law, but it has to be taken into account that the protein content (CP content) of TMV is only 95% (w/w).
6. The CP_{Cys} of TMV_{Cys} has a molecular weight of 17.6 kDa, a maleimide-PEG_{11}-biotin linker molecule ~0.922 kDa. A successful coupling event of a linker molecule to a thiol group of a CP_{Cys} (resulting in CP_{Cys}/Bio) leads to a mass increase up to ~ 18.5 kDa, which results in a distinguishable upward shift of the CP signal upon SDS-PAGE. Therefore, two bands should be visible in these samples. The biotinylation efficiency can be determined by densitometry using ImageJ, given that the amount of CP per band in combination with a colloidal (e.g., Coomassie Blue) stain is in the linear dynamic range of the pixel intensities. The pixel intensity sum of both bands must be set to 100% in order to then calculate the percentage of each fraction (CP_{Cys} or CP_{Cys}/Bio, i.e., faster vs. retarded band).
7. The CP-aggregates devoid of RNA are heterogeneous. After incubation at RT in the buffer applied, they will predominantly contain two-layer (34mer) or four-layer (68mer) disks and oligomers thereof [31]. Before starting the experiment, dilute the CP_{Cys}/Bio-containing solution with 10 mM SPP (pH 7.0) to a concentration of 0.33 μg/μl.
8. Prior to photoresist coating, heat wafer to 180 °C for 5 min to remove adsorbed water from the substrate surface, to allow a better adhesion of the hydrophobic photoresist. The typical thickness of the resist should be about 1.4 μm. Use a soft-bake

step (90 °C for 5 min) to reduce the remaining content of solvent in the resist.

9. Expose the whole wafer to acetone. During this incubation the residual photoresist will be stripped off, together with parts of the metallic thin films covering it. As a result, only the metal layers in direct contact with the underlying SiO_2 surface will remain and form the pattern defined by the applied photomask.
10. A good encapsulation of all bond pads and bond wires is necessary in order to prevent undesired short circuits.
11. Prepare more than one sensor chip in parallel. You can store the sensor chips in 10 mM SPP, pH 7, at 4 °C for several hours/days without bacteriostatic preservatives.
12. The [SA]-GOD solution applied contains 1 μg/μl [SA]-GOD in 0.1 MK-phosphate buffer, pH 6.0, and is supplemented with 10 μg/μl BSA and 1200 ppm 5-nitro-5-bromo-1,3-dioxan. The BSA amount contained in the enzyme solution allows the glutardialdehyde mediated cross-linking without further addition of BSA.
13. While using a potentiostat equipped with eight-channel multiplexer, two sensor chips (in summary eight electrodes) can be characterized in parallel.

References

1. Sassolas A, Blum LJ, Leca-Bouvier BD (2012) Immobilization strategies to develop enzymatic biosensors. Biotechnol Adv 30(3):489–511
2. Brena B, Gonzalez-Pombo P, Batista-Viera F (2013) Immobilization of enzymes: a literature survey. Methods Mol Biol 1051:15–31
3. DiCosimo R, McAuliffe J, Poulose AJ, Bohlmann G (2013) Industrial use of immobilized enzymes. Chem Soc Rev 42(15):6437–6474
4. Singh RK, Tiwari MK, Singh R, Lee JK (2013) From protein engineering to immobilization: promising strategies for the upgrade of industrial enzymes. Int J Mol Sci 14(1):1232–1277
5. Mateo C, Palomo JM, Fernandez-Lorente G, Guisan JM, Fernandez-Lafuente R (2007) Improvement of enzyme activity, stability and selectivity via immobilization techniques. Enzyme Microb Technol 40(6):1451–1463
6. Bäcker M, Koch C, Eiben S, Geiger F, Eber F, Gliemann H et al (2017) Tobacco mosaic virus as enzyme nanocarrier for electrochemical biosensors. Sensors Actuators B Chem 238:716–722
7. Koch C, Wabbel K, Eber FJ, Krolla-Sidenstein P, Azucena C, Gliemann H et al (2015) Modified TMV particles as beneficial scaffolds to present sensor enzymes. Front Plant Sci 6, Article 1137
8. Carette N, Engelkamp H, Akpa E, Pierre SJ, Cameron NR, Christianen PC et al (2007) A virus-based biocatalyst. Nat Nanotechnol 2(4):226–229
9. Chatterji A, Ochoa W, Shamieh L, Salakian SP, Wong SM, Clinton G et al (2004) Chemical conjugation of heterologous proteins on the surface of cowpea mosaic virus. Bioconjug Chem 15(4):807–813
10. Aljabali AA, Barclay JE, Steinmetz NF, Lomonossoff GP, Evans DJ (2012) Controlled immobilisation of active enzymes on the cowpea mosaic virus capsid. Nanoscale 4(18):5640–5645
11. Pille J, Cardinale D, Carette N, Di Primo C, Besong-Ndika J, Walter J et al (2013) General strategy for ordered noncovalent protein assembly on well-defined nanoscaffolds. Biomacromolecules 14(12):4351–4359

12. Cardinale D, Michon T (2016) Enzyme nanocarriers. Pan Standford Publishing, CRC Press, Taylor and Francis Group, Boca Raton, FL
13. Bittner AM, Alonso JM, Gorzny ML, Wege C (2013) Nanoscale science and technology with plant viruses and bacteriophages. Subcell Biochem 68:667–702
14. Culver JN, Brown AD, Zang F, Gnerlich M, Gerasopoulos K, Ghodssi R (2015) Plant virus directed fabrication of nanoscale materials and devices. Virology 479-480:200–212
15. Fan XZ, Pomerantseva E, Gnerlich M, Brown A, Gerasopoulos K, McCarthy M et al (2013) Tobacco mosaic virus: a biological building block for micro/nano/bio systems. J Vac Sci Technol A 31(5) 050815
16. Caspar DL (1963) Assembly and stability of the tobacco mosaic virus particle. Adv Protein Chem 18:37–121
17. Butler PJ (2009) Assembly of tobacco mosaic virus. R Soc Lond B Biol Sci 276(943): 151–163
18. Koch C, Eber FJ, Azucena C, Forste A, Walheim S, Schimmel T et al (2016) Novel roles for well-known players: from tobacco mosaic virus pests to enzymatically active assemblies. Beilstein J Nanotechnol 7:613–629
19. Geiger FC, Eber FJ, Eiben S, Mueller A, Jeske H, Spatz JP et al (2013) TMV nanorods with programmed longitudinal domains of differently addressable coat proteins. Nanoscale 5(9):3808–3816
20. Chen C, Xie Q, Yang D, Xiao H, Fu Y, Tan Y et al (2013) Recent advances in electrochemical glucose biosensors: a review. RSC Adv 3(14):4473–4491
21. Mao C, Liu A, Cao B (2009) Virus-based chemical and biological sensing. Angew Chem 48(37):6790–6810
22. Srinivasan K, Cular S, Bhethanabotla VR, Lee SY, Harris MT, Culver JN (2005) AIChE annual meeting, Cincinnati, USA, p 74d/1
23. Bruckman MA, Liu J, Koley G, Li Y, Benicewicz B, Niu Z et al (2010) Tobacco mosaic virus based thin film sensor for detection of volatile organic compounds. J Mater Chem 20(27):5715–5719
24. Zang F, Gerasopoulos K, Fan XZ, Brown AD, Culver JN, Ghodssi R (2014) An electrochemical sensor for selective TNT sensing based on Tobacco mosaic virus-like particle binding agents. Chem Commun 50(85):12977–12980
25. Fan XZ, Naves L, Siwak NP, Brown A, Culver J, Ghodssi R (2015) Integration of genetically modified virus-like-particles with an optical resonator for selective bio-detection. Nanotechnology 26(20):205501
26. Bäcker M, Delle L, Poghossian A, Biselli M, Zang W, Wagner P et al (2011) Electrochemical sensor array for bioprocess monitoring. Electrochim Acta 56(26):9673–9678
27. Gooding G Jr, Hebert T (1967) A simple technique for purification of tobacco mosaic virus in large quantities. Phytopathology 57(11):1285
28. Zaitlin M, Israel H (1975) Tobacco mosaic virus (type strain). CMI/AAB descriptions of plant viruses. No. 151. http://www.dpvweb.net/
29. Green MR, Sambrook J (2012) Molecular cloning: a laboratory manual, 4th edn. Cold Spring Harbor Laboratory Press, New York
30. Fraenkel-Conrat H (1957) Degradation of tobacco mosaic virus with acetic acid. Virology 4(1):1–4
31. Butler PJ (1984) The current picture of the structure and assembly of tobacco mosaic virus. J Gen Virol 65(Pt 2):253–279